On linking an earth system model to the equilibrium carbon representation of an economically optimizing land use model

Ben Bond-Lamberty[1]*, Katherine Calvin[1], Andrew D. Jones[2], Jiafu Mao[3], Pralit Patel[1], Xiaoying Shi[3], Allison Thomson[1], Peter Thornton[3], and Yuyu Zhou[1]

[1]Joint Global Change Research Institute, Pacific Northwest National Laboratory, College Park, MD, USA

[2]Lawrence Berkeley National Laboratory, 1 Cyclotron Rd., MS 74-0171, Berkeley, CA, USA

[3]Environmental Sciences Division, Oak Ridge National Laboratory, Oak Ridge, TN, USA

* Corresponding author: bondlamberty@pnnl.gov

Submitted to *Geoscientific Model Development*

January 26, 2014

Revised version submitted June 6, 2014

Abstract

Human activities are significantly altering biogeochemical cycles at the global scale, and the scope of these activities will change with both future climate and socioeconomic decisions. This poses a significant challenge for earth system models (ESMs), which can incorporate land-use change as static inputs but do not simulate the

policy or economic forces that drive land use change. One option to address this problem is to couple an ESM with an economically oriented integrated assessment model, but this is challenging because of the radically different goals and underpinnings of each type of model. This study describes the development and testing of a coupling between the terrestrial carbon cycle of an ESM (CESM) and an integrated assessment (GCAM) model, focusing on how CESM climate effects on the carbon cycle can be shared with GCAM. We examine the best proxy variables to share between the models, and quantify how carbon flux changes driven by climate (e.g. CO_2 fertilization) and land-use changes (e.g. deforestation) can be distinguished from each other by GCAM. The net primary production and heterotrophic respiration outputs of the Community Land Model (CLM), the land component of CESM, were found to be the most robust proxy variables by which to manipulate GCAM's assumptions of equilibrium ecosystem steady state carbon. Carbon-cycle effects of land-use change are spatially limited relative to climate effects, and thus we were able to distinguish these effects successfully in the model coupling, passing only the latter to GCAM. This paper does not present results of a fully coupled simulation but shows, using a series of offline CLM simulations and an additional idealized Monte Carlo simulation, that our CESM-GCAM proxy variables reflect the phenomena that we intend, and do not contain erroneous signals due to LUC. By allowing climate effects from a full ESM to dynamically modulate the economic and policy decisions of an integrated assessment model, this work will help link these models in a robust and flexible framework capable of examining two-way interactions between human and earth system processes.

1. Introduction

Human activities are significantly altering biogeochemical cycles at the global scale, e.g. by appropriation of net primary production (Imhoff et al., 2004;Ito, 2011), modification of natural fire dynamics (Pechony and Shindell, 2010), and fossil fuel emissions raising atmospheric CO_2 levels (Le Queré et al., 2009). In addition, land-use change (LUC) exerts strong effects on the global carbon cycle (Bonan, 2008;Caspersen et al., 2000;Arora and Boer, 2010;Laganière et al., 2009), as well as direct biophysical effects on albedo and water vapor fluxes, that in turn have significant regional to global consequences (Brovkin et al., 2013;Jones et al., 2013b). As a result, different policy choices vis-à-vis LUC and carbon may result in greatly different configurations of the future carbon cycle and climate system (Wise et al., 2009;Jones et al., 2013a), even though the direct LUC fluxes will likely be far smaller than in the past (Brovkin et al., 2013).

This poses a significant challenge for global earth system models (ESMs), in which fully coupled climate models are used to draw inferences about Earth's past and future climate states and understand how changes to the radiative properties of Earth's atmosphere interact with its climate, biogeochemistry, and carbon cycle (Brovkin et al., 2013;Todd-Brown et al., 2014). Such models may incorporate LUC as static inputs, but do not simulate policy options or economic forces, a significant limitation given how strongly humans can perturb the earth system (Hurtt et al., 2002;Randerson et al., 2009). Conversely, integrated assessment models (IAMs) are used to examine the human components of the Earth system, including greenhouse gas emission sources, and drivers of land-use change. Their representation of the physical climate and earth system is

simplistic, however, with little spatial resolution or process fidelity compared to an ESM (Meinshausen et al., 2008). These two modeling paradigms—ESMs with no economic or energy system modeling, and IAMs with only basic representations of natural processes—developed largely independently of each other, and their interactions have historically been limited.

ESMs and IAMs increasingly need each other's capabilities, however (van Vuuren et al., 2012;Houghton, 2013). One solution is to couple an ESM to an IAM, letting each model specialize in its specific domain while passing information on the natural and human systems, respectively, between them. This would provide a two-way coupling within a single integrated system, whereby economic decisions in the IAM translate directly into trace gas fluxes and land use changes in the ESM, and changes in the ESM climate feed back onto crop yields, heating and cooling demands, energy production, etc. in the IAM. Successfully linking such complex, large models would permit integrated and unprecedented analyses of the interactions between economic change, climate policy, and the physical earth system, with fully coupled feedbacks between the economic and physical-science components (van Vuuren et al., 2012).

This paper describes the development and testing of a mechanism linking the terrestrial carbon components of an ESM (CESM, the Community Earth System Model) with an IAM (the Global Change Assessment Model, GCAM) (**Figure 1**). The goals of the current study were to develop and test a robust but tractable coupling allowing GCAM LUC projections to respond to changes in the CESM climate and biogeochemical cycles. We focus here on the terrestrial aspect of the CESM-to-GCAM coupling, but this

is only one component of a larger effort to create a more general integrated Earth System Model (iESM) (Jones et al., 2013a) as described above.

2. Materials and Methods

2.1. Model descriptions

Both CESM's Community Land Model (CLM) and GCAM have been extensively described, and here we note only their most relevant aspects (Gent et al., 2011). The terrestrial model in the CESM system, CLM simulates the cycling and land-atmosphere exchange of energy, water, chemical elements, and trace gases. CLM version 4, used in this study, resulted from merging the biophysical framework of CLM v3.5 (Oleson et al., 2008) with the carbon and nitrogen dynamics of the biogeochemistry model Biome-BGC (Thornton et al., 2002;Running and Hunt, 1993). The model incorporates biogeophysics, surface hydrology, biogeochemistry, and dynamic vegetation components (Bonan et al., 2002), whose dynamics have been extensively tested (Shi et al., 2011;Oleson et al., 2008;Lawrence et al., 2008;Mao et al., 2012a;Mao et al., 2012b). Model vegetation is based on plant functional types (PFTs) occupying dynamic fractions of each grid cell (typically 0.25-2° resolution), with each PFT (1 bare ground, 8 tree, 3 shrub, 3 grass, 1 crop) characterized by distinct physiological parameters (Oleson et al., 2010). The model's C and N cycles are closely coupled and include canopy photosynthesis, plant growth and mortality, photosynthate allocation, and subsurface C and N cycling (Thornton et al., 2007); at any point in time, CLM tracks a wide suite of above- and belowground C pools resulting from the integrated effects of these and other (Kloster et al., 2010) processes.

115 The GCAM model, by contrast, is an economic model driven by assumptions
116 about population size and labor productivity that determine potential gross domestic
117 product in each of 14 regions; these regions are further divided by GCAM's agriculture
118 and land-use submodel into 18 agro-ecological zones or AEZs (Monfreda et al., 2009).
119 GCAM originated as the energy-economic MiniCAM model (Edmonds and Reilly,
120 1983), and currently integrates energy, agriculture, forestry, and land markets with a
121 simple terrestrial carbon cycle (Thomson et al., 2010;Wise et al., 2009). The model
122 operates on a 5-year timestep, computing simultaneous market-clearing prices for all
123 energy, agriculture, and land markets (Kim et al., 2006). The model is typically used to
124 explore the effects of policy scenarios–for example, carbon pricing, emissions
125 constraints, or capped limits on total radiative forcing (Calvin et al., 2009). Economic
126 land use decisions are determined by a logit mathematical model, based on the relative
127 inherent profitability of using land for competing purposes. GCAM does not use land use
128 allocation constraints, but its calibration based on historical data means that history is
129 reflected in future land allocation decisions (Wise and Calvin, 2010;Wise et al., 2014).
130 GCAM's carbon model is fundamentally concerned with calculating LUC CO_2
131 emissions resulting from the model's economic decisions. It does this by determining the
132 C stocks changes with every land use change, and allocating those as C fluxes over time.
133 Specifically, each land use (in each AEZ of each political region) has above- (vegetation)
134 and belowground (soil) steady-state C densities associated with it, values currently based
135 on Houghton (1999). These values vary by AEZ and political region and do not change
136 during the model run; i.e., land is assumed to be in C equilibrium with the atmosphere in
137 the absence of LUC. When a particular land-use contracts in area, all the lost

aboveground C (i.e. the land-use's C density multiplied by the change in area) is emitted instantaneously, while its belowground C is emitted in an exponential decay pattern. When a land-use expands, the resulting C uptake depends on the length of time it takes for the vegetation to mature (from 1 yr for crops to 30-100 yr for forests), following a Bertalanffy-Richards growth function. Carbon emission and sequestration thus result only from changes in land use, with emission from shrinking land-uses set against uptake from growing ones. The model computes these fluxes across time but, importantly, does not track current C stocks in the manner of CLM or most land surface models. Further details on the agriculture, land use, and carbon cycle assumptions and algorithms of GCAM may be found in its online documentation (http://wiki.umd.edu/gcam) and several publications (Wise et al., 2014;Wise and Calvin, 2010).

In the iESM architecture a third model, the Global Land Model or GLM (http://eos-webster.sr.unh.edu/data_guides/glm_dg.jsp), currently downscales GCAM's land use decisions (made on agro-ecological zones at the regional level) onto CLM's global grid (**Figure 1**). This step uses algorithms and assumptions described by Di Vittorio et al. (2014) and Lawrence et al. (2012), and is not detailed further here, as this study focuses only on the coupling from CLM to GCAM.

2.2. Issues in linking the CLM and GCAM carbon cycles

The fundamental conceptual, as opposed to technical, problem in linking the CLM and GCAM carbon cycle models is that the former tracks time-varying C pools and fluxes, while the latter bases its economic optimization on long-term (equilibrium) C pools for large regions, and only computes LUC fluxes. Replacing GCAM's entire

161 internal carbon cycle (and its reliance on equilibrium C) may be possible in the long term,
162 but would require a fundamental rewriting of this complex model's agriculture and land-
163 use code. In this study a looser coupling between CLM and GCAM was deemed more
164 tractable, while also sufficient for the experiments described here. Such an approach
165 transmits relative changes between the models while allowing baseline data, against
166 which the models have been calibrated and tested, to differ.

167 Such a 'loose' coupling means that when a CLM grid cell's carbon cycle changes,
168 we need to (i) have a suitable proxy by which to change GCAM's steady-state carbon
169 assumptions, and (ii) distinguish LUC effects on carbon fluxes from climate and other
170 (CO_2, N deposition, etc.) effects, because only the latter should affect GCAM's
171 assumptions of equilibrium C stocks. For example, if the carbon stock of a CLM forest
172 changes from one time step to the next because of harvest, this should not affect GCAM's
173 economic optimization—the forest will regrow to the same equilibrium state. If the same
174 forest's carbon pool rises because of CO_2 fertilization, however, this information (i.e.,
175 there is more C sequestration potential available for this land use type) needs to be
176 propagated to GCAM's assumptions about long-term pool potentials. Distinguishing
177 these sources is thus critical (Gasser and Ciais, 2013).

178

179 *2.3. Identifying the best proxy variables to link CLM to GCAM*

180 Given the decision to adjust GCAM's equilibrium C assumptions based on
181 relative changes in the CLM carbon cycle, one possible proxy variable to pass between
182 the models was CLM's time-varying carbon pools, based on the assumption that short-
183 term pool changes will translate to longer-term (i.e. equilibrium, as needed by GCAM)

184 storage changes. These data may be more vulnerable to LUC effects than carbon flux
185 data, however, as fluxes typically recover much faster from disturbance than do the
186 slower pools (Amiro et al., 2010;Goetz et al., 2012). Short-term changes in C fluxes can
187 be analytically related to steady-state C pools in models, even in the presence of
188 ecosystem disturbances (Hurtt et al., 2010). This needed to be tested and demonstrated
189 for CLM, however.

190 We tested potential proxy variables in two ways. First, we ran a series of single
191 forcing factor experiments in CLM, looking at how changes in each factor affected CLM
192 carbon stocks and fluxes (specifically, gross primary production, net primary production
193 or NPP, heterotrophic respiration or HR, soil organic matter, vegetation carbon, and total
194 ecosystem carbon). The three forcing factors tested were atmospheric CO_2, as alleviating
195 the CO_2 constraints on leaf-level photosynthesis may cascade up to ecosystem carbon
196 storage (Gedalof and Berg, 2010;Lenton and Huntingford, 2003); nitrogen deposition, a
197 potentially strong constraint on the current and future global carbon cycle (Galloway et
198 al., 2005;Norby et al., 2010); and LUC, which affects both immediate and long-term
199 land-atmosphere interactions (Caspersen et al., 2000;Pongratz et al., 2009). A 'good'
200 proxy variable would be strongly affected by the first two CO_2 and N, but not by LUC (as
201 only the former two will affect equilibrium C; see above), and would accurately reflect
202 climate-driven changes to equilibrium C stocks in CLM.

203 In simulation S1 (the control), we used 1901-1920 climate drivers for the entire
204 period 1850-2010, and kept atmospheric CO_2 concentration, nitrogen deposition, and
205 land cover constant at their 1850 values. In simulations S2-S4, we used the same looped
206 climate, and varied one of the three factors in each while holding the other two factors

207 constant (**Table 1**). The time varying factors were based on transient datasets constructed
208 to mimic as closely as possible the historical record over the period 1850-2010, as
209 described by Shi et al. (2013). The effect of each individual factor was then calculated by
210 subtracting S1 from simulations S2, S3 and S4. The CRUNCEP data used to drive these
211 uncoupled simulations is a combination of the CRU TS.2.1 0.5° monthly 1901-2002
212 climatology (Mitchell and Jones, 2005) and the 2.5° NCEP2 reanalysis data beginning in
213 1948 and available in near real time (Kanamitsu et al., 2002;Mao et al., 2012b).

214 Second, we examined how well NPP in particular was related to equilibrium C
215 stocks in CLM only (i.e. before any coupling to GCAM). This involved two offline
216 experiments (**Table 1**) with a repeating 5-year climate drawn either from the beginning
217 (2005-2009, simulation E1) or end (2090-2094, simulation E2) of an RCP4.5 coupled
218 simulation (Taylor et al., 2012). We quantified how well (i) NPP in the first 5 years of
219 simulation E1 predicted total vegetation C in the final 5 years, and (ii) the change in NPP
220 resulting from an altered climate state (E2 minus E1) predicted the relative change in C
221 pools over the final years of the two simulations.

222 Taken together, these experiments tested how well NPP could be used to predict
223 equilibrium C under both constant and changing climate. The state of the terrestrial
224 carbon system at the beginning of these simulations reflected the disturbance and climate
225 histories of the 20th century, with various different non-equilibrium C states across
226 different grid cells and PFTs. Land cover was fixed at 2000 values, and we ran the E1
227 and E2 simulations for 150 model years with no additional LUC in order to allow the
228 carbon stocks to approach their equilibrium state. It is important to note that we did not
229 disable the fire algorithms in CLM. Fire significantly influences model stocks and fluxes

(Li et al., 2014), and thus rather than converging to a single steady-state carbon stock, PFTs influenced by fire converged to a quasi-equilibrium characterized by periodic carbon losses due to fire followed by periods of recovery.

2.4. Distinguishing climate from land-use signals

As noted above, it is important to distinguish carbon cycle changes caused by LUC, versus those caused by climate change. For the CLM to GCAM coupling, even a perfect proxy variable will be subject to climate and LUC during a CESM run, both before the run starts (i.e., during spinup or initialization phases) as well as during a model run. For example, a cell in which a new PFT is established immediately prior to an iESM run would have very low C stocks and NPP in the first timestep; as its vegetation regrows, the cell would appear, to GCAM, to be undergoing enormous productivity increases. Conversely, significant expansion of a PFT (e.g., agriculture reverting to forest) during the iESM run might appear to have drastically lowered productivity, leading GCAM to redirect land away from that PFT. Both of these cases cause problems for GCAM because productivity drives decision-making in the model, which bases its land-use decisions based on the relative inherent profitability of using land for competing purposes (Wise and Calvin, 2010). As a result apparent changes in productivity produce changes in profit (as measured in U.S. dollars) and thus land use.

Thus in both cases, we need to exclude cells with anomalously large C changes, driven by LUC, from the final numeric scalars (i.e., the proxy variables signaling how much GCAM should adjust its assumptions of equilibrium C) computation. They will bias the computation of the scalars, and lead GCAM into a possible feedback loop: if the

253 model sees highly anomalous values, it may allocate more land to those PFTs, resulting
254 in higher profits and further land use change in the region with the anomaly. (A negative
255 feedback is also possible; both cases occur because the changed productivity alters the
256 relative profitability of the different land uses, and profit maximization is the
257 fundamental decision-making criterion in GCAM.)
258 To distinguish LUC from climate signals, we assumed that climate changes will
259 have a broad spatial distribution, either global or regional, while LUC will affect
260 relatively small groups of cells in any particular timestep; this obviously may not hold in
261 particular regions and points in time (Arora and Boer, 2010), but should be broadly true
262 across the millions of data points (~10^5 grid cells x PFT combinations) being output by
263 CLM. Thus a statistical outlier test, comparing how much any particular cell's carbon
264 cycle has changed relative to the start of the run, should be able to exclude cells whose
265 inferred change in long-term carbon density fall significantly outside of the norm. To do
266 so we used a method based on median absolute deviation (Davies and Gather, 1993), a
267 robust (insensitive to outliers) measure of central tendency. The scalars were then
268 mapped from CLM's PFTs and grid cells to GCAM's land-cover types and AEZ regions,
269 weighted by PFT area, land area in each grid cell, and cell area in the AEZ.
270 This technique depends on the overall population mean not being overly
271 perturbed, and thus will not work in extreme scenarios of mass deforestation (e.g., Bonan
272 et al., 1992). An important question is how soon, under increasing amounts of LUC, bias
273 (i.e., LUC effects masquerading as climate change to GCAM) will be introduced into the
274 iESM model system. We used a Monte Carlo simulation (M1 in **Table 1**), written in the
275 statistical package R 2.15.1 (R Development Core Team, 2012), to examine how robust

this outlier exclusion method would be to different levels of LUC, and what if any bias it might introduce to the GCAM carbon density values. For this exercise, 10,000 cells were simulated in which a constant +10% climate-change effect on equilibrium C was presumed to be occurring (Jain and Yang, 2005). A LUC effect, ranging from -500% to +500% and affecting from 5% to 95% of the cells, was then additionally applied. The outlier exclusion test defined above was then calculated on the cells, and a putative signal calculated on the remaining cells. This inferred climate change was then compared to the original known climate signal to quantify how much error would be introduced into iESM under such circumstances.

3. Results and Discussion

3.1. Single-forcing tests: identifying the best proxy variables

Clear differences emerged between the potential proxy variables tested in CLM in response to three different forcing factors (**Figure 2**). Most notably, carbon stocks were much more sensitive to LUC than were carbon fluxes. This result matches both theory (Odum, 1969) and a wide variety of field studies (Amiro et al., 2010;Goetz et al., 2012): stocks are by their nature integrative and accumulate relatively slowly compared to C flux changes. In contrast, the C flux variables were highly sensitive to climate effects, but exhibited low sensitivity to LUC.

A second, related problem arising from the use of carbon stocks as proxy variables can be seen in **Figure 3**. In this case a test coupling between CLM and GCAM, using carbon stocks to pass climate-change information, produced sharp and unrealistic changes from the GCAM RCP4.5 control run. (This occurred even when running the

299 outlier-exclusion protocol described above.) Global LUC emissions climbed throughout
300 the 21st century in a departure from the RCP4.5 control, because a few CLM grid cells,
301 located in GCAM's "Middle East" region, were subject to LUC at the end of CLM's
302 spinup phase. As a result, their C stocks (and GCAM's estimation of their long-term
303 potential C) increased rapidly in the early years of the model run, leading GCAM to pour
304 more resources into these cells (because these cells' productivity appeared extraordinarily
305 high, as described in the Methods). Increasing the area of newly planted bioenergy crops
306 created an even stronger signal of rapidly increasing carbon stocks, exacerbating the
307 original problem and causing GCAM to put even more resources into the region. By the
308 end of the century, GCAM was mistakenly growing a huge percentage of the world's
309 bioenergy crops in the region, on a very small area of land (**Figure 3**). Conversely, the
310 use of NPP and HR caused no such problems, because of their relatively fast recovery
311 from LUC disturbance (**cf. Figure 2**).

312 The two primary fluxes determining carbon balance (net primary production and
313 heterotrophic respiration, NPP and HR) were thus chosen as proxy variables linking
314 CLM to GCAM, with CLM NPP changes used to scale GCAM's assumptions of
315 aboveground equilibrium C, while a combination of NPP and HR provided a relative
316 scaling for GCAM's belowground carbon:

$$C_A = C_A \frac{NPP_i}{NPP_0} \quad (1)$$

$$C_B = C_B \left[\frac{NPP_i}{NPP_0} + \frac{HR_0}{HR_i}\right]/2 \quad (2)$$

317 Here the ratio of NPP at time step *i* to NPP at the beginning of the run (NPP_0) determines
318 how aboveground equilibrium C in GCAM (C_A) will change. CLM's NPP and HR

319 together determine changes in GCAM equilibrium belowground carbon (C_B); note that as
320 NPP and HR get larger/smaller and smaller/larger compared to their starting values,
321 GCAM's equilibrium C rises/falls.
322
323 *3.2. Correlation between NPP and equilibrium pools in CLM*
324 Simulations E1 and E2 provided insight into the relationship between NPP and
325 equilibrium C pools within CLM. NPP at the beginning of the E1 simulation was a good
326 predictor of the equilibrium pools values at the end of the simulation (**Figure 4**), although
327 the slope of this relationship varied for different PFTs. It was also apparent that this
328 relationship breaks down at very low NPP values for some PFTs. This result is consistent
329 with ecological theory and observations, as freshly disturbed ecosystems require a period
330 of initial growth before NPP stabilizes. These very low NPP values were reliably
331 excluded by the outlier exclusion method discussed above and tested below.
332 We also found that the change in NPP resulting from an altered pattern of climate
333 (comparing simulations E1 and E2) was a relatively good predictor of the subsequent
334 change in equilibrium C stocks. **Table 2** shows the slopes of the linear relationships
335 between the change in initial NPP (simulation E2 minus E1) and change in equilibrium C
336 for each PFT in CLM. The initial change in NPP was able to explain 20-92% of the
337 variance in the C pool change over the 21st century simulation. In general, NPP was a
338 better predictor for relatively high-carbon forest ecosystems, as compared to grasses,
339 shrubs, and crops. This is good, as high-C systems are particularly important for GCAM:
340 changes in their land areas exert disproportionate effects on atmospheric CO_2, which the
341 model is frequently trying to minimize.

342 To determine whether fire dynamics were responsible for some of the
343 unexplained variance in equilibrium C pools, we performed the same analysis a second
344 time, excluding PFT-gridcell combinations in which the cumulative carbon loss from fire
345 over the 150 year E1 simulation exceeded 800 g C m^{-2}. This led to moderate
346 improvements in the R^2 values in all PFTs except the two broadleaf evergreen PFTs, and
347 moderate increases in the regression slopes, indicating that fire-influenced regions tend to
348 have lower C values than others. This is consistent with both observations and CLM's
349 general fire characteristics (Li et al., 2014). This finding–that the relationship between
350 NPP and equilibrium pools is improved by excluding fire-influenced regions–suggests
351 that fire dynamics and fire regime changes in response to climate change are important to
352 account for when constructing simple proxies that can predict changes in future terrestrial
353 carbon stocks based on evolving climatic and ecological conditions.
354
355 *3.3. Distinguishing LUC from climate*
356 The initial experiments thus established the best available variables to loosely
357 couple CESM and GCAM. But how well could the coupling—specifically, statistically
358 excluding CLM grid cells whose carbon fluxes were changing 'too fast'—separate LUC
359 and climate signals? The M1 experiment results (**Figure 5**) suggested that as long as
360 fewer than ~25% of the simulation cells were perturbed, the error (between the known
361 climate signal and that inferred by the outlier test) remained small (<10%). Even when
362 larger numbers of cells were perturbed, the LUC effect had to be quite large to exceed
363 this level. Because the outlier test is applied to the global population, and not sub-regions,
364 this implies that only under extreme scenarios will this mechanism start to introduce

365 substantial error. (In test iESM runs attempting to reproduce RCP 4.5, 4-8% of the global
366 grid cells were excluded–i.e., failed the outlier test–at each timestep.)
367
368 *3.4. Implications of the loose coupling between CLM and GCAM*
369 For the initial construction of the iESM system, we chose a 'loose' coupling
370 between the ESM and IAM, in which GCAM's equilibrium C assumptions of various
371 ecosystems tracked the *relative* changes in CLM's short-term C fluxes, after exclusion of
372 LUC effects. This has the advantage of not requiring a fundamental rewriting of GCAM,
373 as the mathematical formulae and economic principles underlying its land-use decisions
374 are based on equilibrium C (Wise and Calvin, 2010). In addition, it guarantees that if
375 climate changes affect the carbon cycle, GCAM's equilibrium assumptions will change
376 correspondingly for the same vegetation type and spatial location, feeding back into
377 economic decisions about industrial and LUC CO_2 emissions (e.g., Le Page et al., 2013),
378 emissions that propagate back to CLM (Di Vittorio et al., 2014).
379 This is a powerful improvement over the fixed assumptions of both IAMs and
380 ESMs in these areas, sidestepping the lack of process fidelity and spatial resolution (for
381 the IAM) and addressing the lack of human agency (for the ESM). The loose coupling
382 does have disadvantages, however, requiring the statistical identification of outlier grid
383 cells and inevitable mismatches between the models' definitions of PFTs, C pools, and
384 time steps (Di Vittorio et al., 2014). In addition, the outlier-exclusion step will break
385 down under extreme LUC scenarios, scenarios that can be a useful tool (Bonan,
386 2008;Nobre et al., 1991;Thomson et al., 2010). For these reasons, we anticipate that the
387 long-term solution is a full incorporation of an IAM into an ESM, with a unified C cycle.

4. Conclusions

Here we have implemented and tested a coupling mechanism between the carbon cycles of an earth system model (CLM) and an integrated assessment (GCAM) model. CLM's net primary production and heterotrophic respiration outputs were found to be the most robust proxy variables by which to manipulate GCAM's assumptions of long-term ecosystem steady state carbon, with short-term forest NPP shifts strongly correlated with long-term biomass changes in particular. By assuming the carbon cycle effects of land-use change are short-term and spatially limited relative to widely distributed climate effects, we were able to distinguish these effects successfully in the model coupling, passing only the latter to GCAM. Increasingly extreme LUC scenarios will eventually break down this mechanism, however.

This work is only one step to a full coupling of an ESM and IAM; the second is described by Di Vittorio et al. (Di Vittorio et al., 2014). By allowing climate effects on the CLM carbon cycle to modulate, in real time, the economic and policy decisions of an integrated assessment model, it provides a foundation for further development of the iESM project linking these models in a robust and flexible framework. Such a framework will, in turn, facilitate future modeling of the two-way interactions between human and earth system processes.

Acknowledgements

We are grateful to the DOE Office of Science Integrated Assessment Research Program and Earth System Modeling Program for funding through the integrated Earth

411 System Modeling Project. This research used resources of the National Energy Research
412 Scientific Computing Center, which is supported by the Office of Science of the U.S.
413 Department of Energy under Contract DE-AC02-05CH11231. The CESM project is sup-
414 ported by the National Science Foundation and the Office of Science (Biological and
415 Environmental Research) of the U.S. Department of Energy. We thank S. Smith for his
416 thoughtful comments on an early draft.
417

418 **References**

419 Amiro, B. D., Barr, A. G., Barr, J. G., Black, T. A., Bracho, R., Brown, M., Chen, J. M.,
420 Clark, K. L., Davis, K. J., Desai, A. R., Dore, S., Engel, V., Fuentes, J. D.,
421 Goldstein, A. H., Goulden, M. L., Kolb, T. E., Lavigne, M. B., Law, B. E.,
422 Margolis, H. A., Martin, T. A., McCaughey, J. H., Misson, L., Montes-Helu, M.
423 C., Noormets, A., Randerson, J. T., Starr, G., and Xiao, J.: Ecosystem carbon
424 dioxide fluxes after disturbance in forests of North America, J. Geophys. Res.-
425 Biogeosci., 115, G00K02, 10.1029/2010JG001390, 2010.
426 Arora, V., and Boer, G. J.: Uncertainties in the 20th century carbon budget associated
427 with land use change, Global Change Biol., 16, 3327-3348, 10.1111/j.1365-
428 2486.2010.02202.x, 2010.
429 Bonan, G. B., Pollard, D., and Thompson, S. L.: Effects of boreal forest vegetation on
430 global climate, Nature, 359, 716-718, 1992.
431 Bonan, G. B., Oleson, K. W., Vertenstein, M., Levis, S., Zeng, X. B., Dai, Y., Dickinson,
432 R. E., and Yang, Z.-L.: The land surface climatology of the community land
433 model coupled to the NCAR community climate model, J. Climate, 15, 3123-

3149, 2002.

Bonan, G. B.: Forests and climate change: forcings, feedbacks, and the climate benefits of forests, Science, 320, 1444-1449, 10.1126/science.1155121, 2008.

Brovkin, V., Boysen, L., Arora, V., Boisier, J. P., Cadule, P., Chini, L., Claussen, M., Friedlingstein, P., Gayler, V., van den Hurk, B. J. J. M., Hurtt, G. C., Jones, C. D., Kato, E., de Noblet-Ducoudré, N., Pacifico, F., Pongratz, J., and Weiss, M. S.: Effect of anthropogenic land-use and land-cover changes on climate and land carbon storage in CMIP5 projections for the twenty-first century, J. Climate, 26, 6859-6881, 10.1175/JCLI-D-12-00623.1, 2013.

Calvin, K. V., Edmonds, J. A., Bond-Lamberty, B., Clarke, L. E., Kim, S. H., Kyle, G. P., Smith, S. J., Thomson, A. M., and Wise, M.: 2.6: Limiting climate change to 450 ppm CO_2 equivalent in the 21st century, Energy Economics, 31, S107-S120, 10.1016/j.eneco.2009.06.006, 2009.

Caspersen, J. P., Pacala, S. W., Jenkins, J. C., Hurtt, G. C., Moorcroft, P. R., and Birdsey, R. A.: Contributions of land-use history to carbon accumulation in U.S. forests, Science, 290, 1148-1151, 10.1126/science.290.5494.1148, 2000.

Davies, L., and Gather, U.: The identification of multiple outliers, Journal of the American Statistical Association, 88, 782-792, 1993.

Di Vittorio, A. V., Chini, L., Bond-Lamberty, B., Mao, J., Shi, X., Truesdale, J., Branstetter, M. L., Collins, W. D., Thornton, P. E., Edmonds, J. A., Thomson, A. M., Hurtt, G. C., Calvin, K. V., Jones, A. D., and Craig, T.: From land use to land cover: Restoring the afforestation signal in GCAM to CESM land coupling and the implications for CMIP5 RCP simulations, Biogeosciences, in prep, 2014.

457 Edmonds, J. A., and Reilly, J.: A long-term global energy-economic model of carbon
458 dioxide release from fossil fuel use, Energy Economics, 5, 74-88, 1983.
459 Galloway, J. N., Townsend, A. R., Erisman, J. W., Bekunda, M., Cai, Z., Freney, J. R.,
460 Martinelli, L. A., Seitzinger, S. P., and Sutton, M. A.: Transformation of the
461 nitrogen cycle: recent trends, questions, and potential solutions, Science, 320,
462 889-892, 10.1126/science.1136674, 2005.
463 Gasser, T., and Ciais, P.: A theoretical framework for the net land-to-atmosphere CO2
464 flux and its implications in the definition of "emissions from land-use change",
465 Earth System Dynamics Discussions, 4, 179-217, 10.5194/esdd-4-179-2013,
466 2013.
467 Gedalof, Z. e., and Berg, A. A.: Tree ring evidence for limited direct CO2 fertilization of
468 forests over the 20th century, Glob. Biogeochem. Cycles, 24, GB3027,
469 10.1029/2009GB003699, 2010.
470 Gent, P. R., Danabasoglu, G., Donner, L. J., Holland, M. M., Hunke, E. C., Jayne, S. R.,
471 Lawrence, D. M., Neale, R. B., Rasch, P. J., Vertenstein, M., Worley, P. H.,
472 Yang, Z.-L., and Zhang, M.: The Community Climate System Model Version 4, J.
473 Climate, 24, 4973-4991, 10.1175/2011JCLI4083.1, 2011.
474 Goetz, S. J., Bond-Lamberty, B., Harmon, M. E., Hicke, J. A., Houghton, R. A.,
475 Kasischke, E. S., Law, B. E., McNulty, S. G., Meddens, A. J. H., Mildrexler, D.,
476 O'Halloran, T. L., and Pfeifer, E. M.: Observations and assessment of forest
477 carbon recovery following disturbance in North America, J. Geophys. Res.-
478 Biogeosci., 117, G02022, 10.1029/2011JG001733, 2012.
479 Houghton, R. A.: The annual net flux of carbon to the atmosphere from changes in land

use 1850–1990, Tellus, 51, 298-313, 10.1034/j.1600-0889.1999.00013.x, 1999.

Houghton, R. A.: Keeping management effects separate from environmental effects in terrestrial carbon accounting, Global Change Biol., 19, 2609-2612, 10.1111/gcb.12233, 2013.

Hurtt, G. C., Pacala, S. W., Moorcroft, P. R., Caspersen, J. P., Shevliakova, E., Houghton, R. A., and Moore III, B.: Projecting the future of the U.S. carbon sink, Proc. Nat. Acad. Sci., 99, 1389-1394, 10.1073/pnas.012249999, 2002.

Hurtt, G. C., Fisk, J. P., Thomas, R. Q., Dubayah, R. O., Moorcroft, P. R., and Shugart, H. H.: Linking models and data on vegetation structure, J. Geophys. Res.-Biogeosci., 115, G00E10, 10.1029/2009JG000937, 2010.

Imhoff, M. L., Bouana, L., Ricketts, T., Loucks, C., Harriss, R. C., and Lawrence, W. T.: Global patterns in human consumption of net primary production, Nature, 429, 870-873, 10.1038/nature02619, 2004.

Ito, A.: A historical meta-analysis of global terrestrial net primary productivity: Are estimates converging?, Global Change Biol., 17, 3161-3175, 10.1111/j.1365-2486.2011.02450.x, 2011.

Jain, A. K., and Yang, X.: Modeling the effects of two different land cover change data sets on the carbon stocks of plants and soils in concert with CO2 and climate change, Glob. Biogeochem. Cycles, 19, GB2015, 10.1029/2004GB002349, 2005.

Jones, A. D., Collins, W. D., Edmonds, J. A., Torn, M. S., Janetos, A. C., Calvin, K. V., Thomson, A. M., Chini, L., Mao, J., Shi, X., Thornton, P. E., Hurtt, G. C., and Wise, M.: Greenhouse gas policies influence climate via direct effects of land use change, J. Climate, 26, 3657-3670, 10.1175/JCLI-D-12-00377.1, 2013a.

503 Jones, A. D., Collins, W. D., and Torn, M. S.: On the additivity of radiative forcing
504 between land use change and greenhouse gases, Geophys. Res. Lett., 40, 4036-
505 4041, 10.1002/grl.50754, 2013b.
506 Kanamitsu, M., Ebisuzaki, W., Woollen, J., Yang, S.-K., Hnilo, J. J., Fiorino, M., and
507 Potter, G. L.: NCEP–DOE AMIP-II Reanalysis (R-2), Bulletin of the American
508 Meteorological Society, 83, 1631-1643, 10.1175/BAMS-83-11-1631, 2002.
509 Kim, S. H., Edmonds, J. A., Lurz, J., Smith, S. J., and Wise, M.: The O^{bj}ECTS
510 framework for integrated assessment: Hybrid modeling of transportation, Energy
511 Journal, 27, 63-91, 2006.
512 Kloster, S., Nahowald, N. M., Randerson, J. T., Thornton, P. E., Hoffman, F. M., Levis,
513 S., Lawrence, P. J., Feddema, J. J., Oleson, K. W., and Lawrence, D. M.: Fire
514 dynamics during the 20th century simulated by the Community Land Model,
515 Biogeosciences, 7, 1877-1902, 10.5194/bg-7-1877-2010, 2010.
516 Laganière, J., Angers, D. A., and Paré, D.: Carbon accumulation in agricultural soils after
517 afforestation: a meta-analysis, Global Change Biol., 16, 439-453, 10.1111/j.1365-
518 2486.2009.01930.x, 2009.
519 Lawrence, D. M., Slater, A. G., Romanovsky, V. E., and Nicolsky, D. J.: Sensitivity of a
520 model projection of near-surface permafrost degradation to soil column depth and
521 representation of soil organic matter, J. Geophys. Res., 113, F02011,
522 10.1029/2007jf000883, 2008.
523 Lawrence, P. J., Feddema, J. J., Bonan, G. B., Meehl, G. A., O'Neill, B. C., Oleson, K.
524 W., Levis, S., Lawrence, D. M., Kluzek, E., Lindsay, K., and Thornton, P. E.:
525 Simulating the biogeochemical and biogeophysical impacts of transient land

cover change and wood harvest in the Community Climate System Model (CCSM4) from 1850 to 2100, J. Climate, 25, 3071-3095, 10.1175/JCLI-D-11-00256.1, 2012.

Le Page, Y., Hurtt, G. C., Thomson, A. M., Bond-Lamberty, B., Patel, P., Wise, M., Calvin, K. V., Kyle, G. P., Clarke, L. E., Edmonds, J. A., and Janetos, A. C.: Sensitivity of climate mitigation strategies to natural disturbances, Environ. Res. Lett., 8, 015018, 10.1088/1748-9326/8/1/015018, 2013.

Le Queré, C., Raupach, M. R., Canadell, J. G., Marland, G., Bopp, L., Ciais, P., Conway, T. J., Doney, S. C., Feely, R. A., Foster, P., Friedlingstein, P., Gurney, K. R., Houghton, R. A., House, J. I., Huntingford, C., Levy, P. E., Lomas, M. R., Majkut, J., Metzl, N., Ometto, J. P., Peters, G. P., Prentice, I. C., Randerson, J. T., Running, S. W., Sarmiento, J. L., Schuster, U., Sitch, S., Takahashi, T., Viovy, N., van der Werf, G. R., and Woodward, F. I.: Trends in the sources and sinks of carbon dioxide, Nature Geoscience, 2, 831-836, 10.1038/ngeo689, 2009.

Lenton, T. M., and Huntingford, C.: Global terrestrial carbon storage and uncertainties in its temperature sensitivity examined with a simple model Global Change Biol., 9, 1333-1352, 2003.

Li, F., Bond-Lamberty, B., and Levis, S.: Quantifying the role of fire in the Earth system – Part 2: Impact on the net carbon balance of global terrestrial ecosystems for the 20th century, Biogeosciences, 11, 1345-1360, 10.5194/bg-11-1345-2014, 2014.

Mao, J., Shi, X., Thornton, P. E., Piao, S., and Wang, X.: Causes of spring vegetation growth trends in the northern mid-high latitudes from 1982 to 2004, Environ. Res. Lett., 7, 014010, 10.1088/1748-9326/7/1/014010, 2012a.

549 Mao, J., Thornton, P. E., Shi, X., Zhao, M., and Post, W. M.: Remote sensing evaluation
550 of CLM4 GPP for the period 2000–09, J. Climate, 25, 5327-5342, 10.1175/JCLI-
551 D-11-00401.1, 2012b.
552 Meinshausen, M., Raper, S. C. B., and Wigley, T. M. L.: Emulating IPCC AR4
553 atmosphere-ocean and carbon cycle models for projecting global-mean,
554 hemispheric and land/ocean temperatures: MAGICC 6.0, Atmos. Chem. Phys., 8,
555 6153-6272, 2008.
556 Mitchell, T. D., and Jones, P. D.: An improved method of constructing a database of
557 monthly climate observations and associated high-resolution grids, Internat. J.
558 Climat., 25, 693-712, 2005.
559 Monfreda, C., Ramankutty, N., and Hertel, T.: Global agricultural land use data for
560 climate change analysis, in: Economic Analysis of Land Use in Global Climate
561 Change Policy, edited by: Hertel, T., Rose, S. K., and Tol, R., Routledge, New
562 York, 368, 2009.
563 Nobre, C. A., Sellers, P. J., and Shukla, J.: Amazonian deforestation and regional climate
564 change, J. Climate, 4, 957-988, 1991.
565 Norby, R. J., Warren, J. M., Iversen, C. M., Medlyn, B. E., and McMurtrie, R. E.: CO2
566 enhancement of forest productivity constrained by limited nitrogen availability,
567 Proc. Nat. Acad. Sci., 107, 19368-19373, 10.1073/pnas.1006463107, 2010.
568 Odum, E. P.: The strategy of ecosystem development, Science, 164, 262-270,
569 10.1126/science.164.3877.262, 1969.
570 Oleson, K. W., Niu, G.-Y., Yang, Z.-L., Lawrence, D. M., Thornton, P. E., Lawrence, P.
571 J., Stöckli, R., Dickinson, R. E., Bonan, G. B., Levis, S., Dai, A., and Qian, T.:

572 Improvements to the Community Land Model and their impact on the
573 hydrological cycle, J. Geophys. Res.-Atmos., 113, G01021,
574 10.1029/2007JG000563, 2008.
575 Oleson, K. W., Lawrence, D. M., Bonan, G. B., Flanner, M. G., Kluzek, E., Lawrence, P.
576 J., Levis, S., Swenson, S. C., Thornton, P. E., Dai, A., Decker, M., Dickinson, R.
577 E., Feddema, J. J., Heald, C. L., Hoffman, F. M., Lamarque, J. F., Mahowald, N.
578 M., Niu, G.-Y., Qian, T., Randerson, J. T., Running, S. W., Sakaguchi, K., Slater,
579 A. G., Stöckli, R., Wang, A., Yang, Z.-L., Zeng, X., and Zeng, X.: Technical
580 Description of version 4.0 of the Community Land Model (CLM), National
581 Center for Atmospheric Research, Boulder, 257, 2010.
582 Pechony, O., and Shindell, D. T.: Driving forces of global wildfires over the past
583 millennium and the forthcoming century, Proc. Nat. Acad. Sci., 107, 19167-
584 19170, 10.1073/pnas.1003669107, 2010.
585 Pongratz, J., Reick, C. H., Raddatz, T. J., and Claussen, M.: Effects of anthropogenic
586 land cover change on the carbon cycle of the last millennium, Glob. Biogeochem.
587 Cycles, 23, GB4001, 10.1029/2009GB003488., 2009.
588 Randerson, J. T., Hoffman, F. M., Thornton, P. E., Mahowald, N. M., Lindsay, K., Lee,
589 Y.-H., Nevison, C. D., Doney, S. C., Bonan, G. B., Stöckli, R., Covey, C.,
590 Running, S. W., and Fung, I. Y.: Systematic assessment of terrestrial
591 biogeochemistry in coupled climate–carbon models, Global Change Biol., 15,
592 2462-2484, 10.1111/j.1365-2486.2009.01912.x, 2009.
593 Running, S. W., and Hunt, R. E.: Generalization of a forest ecosystem process model for
594 other biomes, BIOME-BGC, and an application for global-scale models, in:

595 Scaling Physiologic Processes: Leaf to Globe, edited by: Ehleringer, J. R., and
596 Field, C. B., Academic Press, San Diego, CA, 141-158, 1993.
597 Shi, X., Mao, J., Thornton, P. E., Hoffman, F. M., and Post, W. M.: The impact of
598 climate, CO_2, nitrogen deposition and land use change on simulated contemporary
599 global river flow, Geophys. Res. Lett., 38, L08704, 10.1029/2011GL046773,
600 2011.
601 Shi, X., Mao, J., Thornton, P. E., and Huang, M.: Spatiotemporal patterns of
602 evapotranspiration in response to multiple environmental factors simulated by the
603 Community Land Model, Environ. Res. Lett., 8, 024012, 10.1088/1748-
604 9326/8/2/024012, 2013.
605 Taylor, K. E., Stouffer, R. J., and Meehl, G. A.: An overview of CMIP5 and the
606 experiment design, Bulletin of the American Meteorological Society, 93, 485-
607 498, 10.1175/BAMS-D-11-00094.1, 2012.
608 Thomson, A. M., Calvin, K. V., Chini, L., Hurtt, G. C., Edmonds, J. A., Bond-Lamberty,
609 B., Frolking, S. E., Wise, M., and Janetos, A. C.: Climate mitigation and the
610 future of tropical landscapes, Proc. Nat. Acad. Sci., 107, 19633-19638,
611 10.1073/pnas.0910467107, 2010.
612 Thornton, P. E., Law, B. E., Gholz, H. L., Clark, K. L., Falge, E., Ellsworth, D. S.,
613 Goldstein, A. H., Monson, R. K., Hollinger, D. Y., Falk, M., Chen, J., and Sparks,
614 J. P.: Modeling and measuring the effects of disturbance history and climate on
615 carbon and water budgets in evergreen needleleaf forests, Agric. Forest Meteorol.,
616 113, 185-222, 10.1016/S0168-1923(02)00108-9, 2002.
617 Thornton, P. E., Lamarque, J.-F., Rosenbloom, N. A., and Mahowald, N. M.: Influence of

carbon-nitrogen cycle coupling on land model response to CO2 fertilization and climate variability, Glob. Biogeochem. Cycles, 21, Art. No. GB4018, 10.1029/2006GB002868, 2007.

Todd-Brown, K. E. O., Randerson, J. T., Hopkins, F. M., Arora, V., Hajima, T., Jones, C. D., Shevliakova, E., Tjiputra, J., Volodin, E. M., Wu, T., Zhang, Q., and Allison, S. D.: Changes in soil organic carbon storage predicted by Earth system models during the 21st century, Biogeosciences, 11, 2341-2356, 10.5194/bgd-10-18969-2013, 2014.

van Vuuren, D. P., Bayer, L. B., Chuwah, C., Ganzeveld, L., Hazeleger, W., van den Hurk, B. J. J. M., van Noije, T., O'Neill, B. C., and Strengers, B. J.: A comprehensive view on climate change: coupling of earth system and integrated assessment models, Environ. Res. Lett., 7, 024012, 10.1088/1748-9326/7/2/024012, 2012.

Wise, M., Calvin, K. V., Thomson, A. M., Clarke, L. E., Bond-Lamberty, B., Sands, R. D., Smith, S. J., Janetos, A. C., and Edmonds, J. A.: Implications of limiting CO_2 concentrations for land use and energy, Science, 324, 1183-1186, 10.1126/science.1168475, 2009.

Wise, M., and Calvin, K. V.: GCAM 3.0 Agriculture and Land Use: Technical Description of Modeling Approach, Pacific Northwest National Laboratory PNNL-20971 (https://wiki.umd.edu/gcam/images/8/87/GCAM3AGTechDescript12_5_11.pdf), 2010.

Wise, M., Calvin, K. V., Kyle, G. P., Luckow, P., and Edmonds, J. A.: Economic and

641 physical modeling of land use in GCAM 3.0 and an application to agricultural
642 productivity, land, and terrestrial carbon, Climate Change Economics, in press,
643 2014.
644
645

646 **Table 1.** Summary of simulations performed.

Name	Type	Purpose
S1	Uncoupled CLM, 1850-2010, constant (1901-1920) climate	Control for S2, S3, S4
S2	S1 + changing CO_2	Single-factor experiments quantifying how CO_2, N deposition, and LUC affect potential proxy variables
S3	S1 + changing N deposition	
S4	S1 + changing LUC	
E1	Uncoupled CLM, constant (2005-2009) climate	Equilibrium biomass simulations quantifying how initial NPP predicts final vegetation C
E2	Uncoupled CLM, constant (2090-2094) climate	Equilibrium biomass simulation quantifying how climate-driven changes in NPP predict changes in vegetation C
M1	Idealized Monte Carlo	Assess error that could be introduced to climate effects scalars by increasing amount of LUC.

647

648

649 **Table 2.** Slope (yr), adjusted R^2 value, and number of grid cells for the relationship
650 between change in NPP in response to a climate change signal and resulting change in
651 equilibrium biomass (simulations E1 and E2 in **Table 1**). Excluding PFTs whose
652 cumulative carbon loss from fires exceeds 8 Mg C ha^{-1} over 150 years generally
653 improved the R^2 values and increased the slopes (data not shown).

PFT	Name	Slope	R^2	Count
1	needleleaf_evergreen_temperate_tree	20.4	0.52	3500
2	needleleaf_evergreen_boreal_tree	20.5	0.68	5136
3	needleleaf_deciduous_boreal_tree	24.9	0.92	1643
4	broadleaf_evergreen_tropical_tree	18.0	0.35	2609
5	broadleaf_evergreen_temperate_tree	20.9	0.40	1702
6	broadleaf_deciduous_tropical_tree	25.2	0.56	3909
7	broadleaf_deciduous_temperate_tree	21.9	0.49	3966
8	broadleaf_deciduous_boreal_tree	23.6	0.64	5311
	All trees	*21.5*	*0.51*	*27776*
9	broadleaf_evergreen_shrub	1.9	0.06	299
10	broadleaf_deciduous_temperate_shrub	5.8	0.45	3336
11	broadleaf_deciduous_boreal_shrub	6.5	0.60	5979
	All shrubs	*6.0*	*0.50*	*9614*
12	c3_arctic_grass	1.8	0.30	6417
13	c3_non-arctic_grass	2.4	0.38	8061
14	c4_grass	1.1	0.19	5436
	All grasses	*1.6*	*0.28*	*19914*

15	crop	1.7	0.19	9142

654

655

Figure 1. High-level overview of the iESM (integrated earth system model) system; a more detailed schematic is presented by Di Vittorio et al (2014). Oval boxes represent models, and arrows show data flows. This paper focuses on the information flow between CLM (part of CESM) and GCAM, in bold.

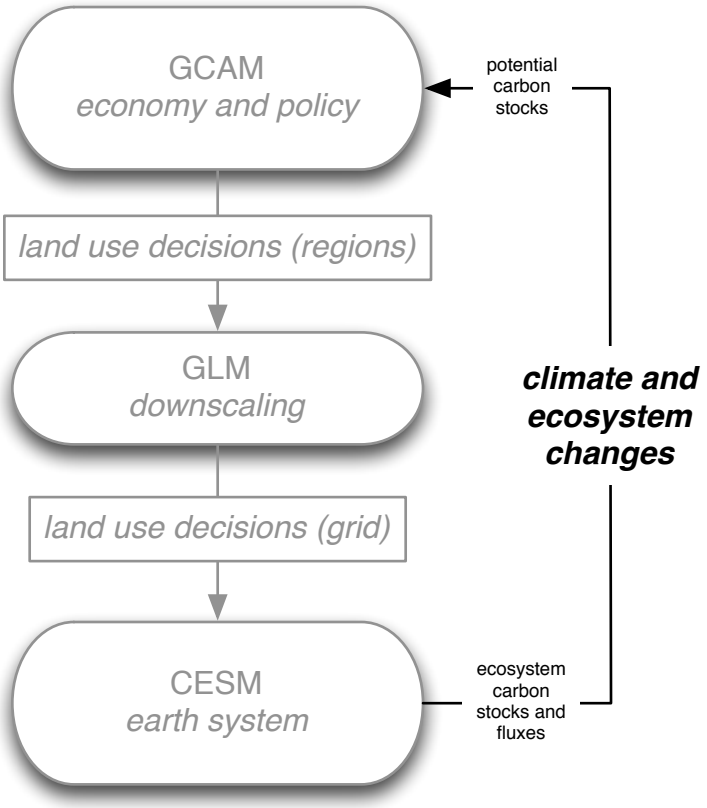

Figure 2. Response of Community Land Model outputs to changes in atmospheric CO_2 (simulation S2), nitrogen deposition (NDEP, simulation S3), and land-use/land cover change (LULLC, simulation S4; cf. **Table 1**). Outputs shown are all relative to an 1850 baseline, as described in the text, and include fire emissions (Fire), terrestrial gross primary production (GPP), heterotrophic respiration (HR), net primary production (NPP), carbon in soil organic matter (SOMC), total ecosystem carbon (TOTC), and total vegetation carbon (VegC).

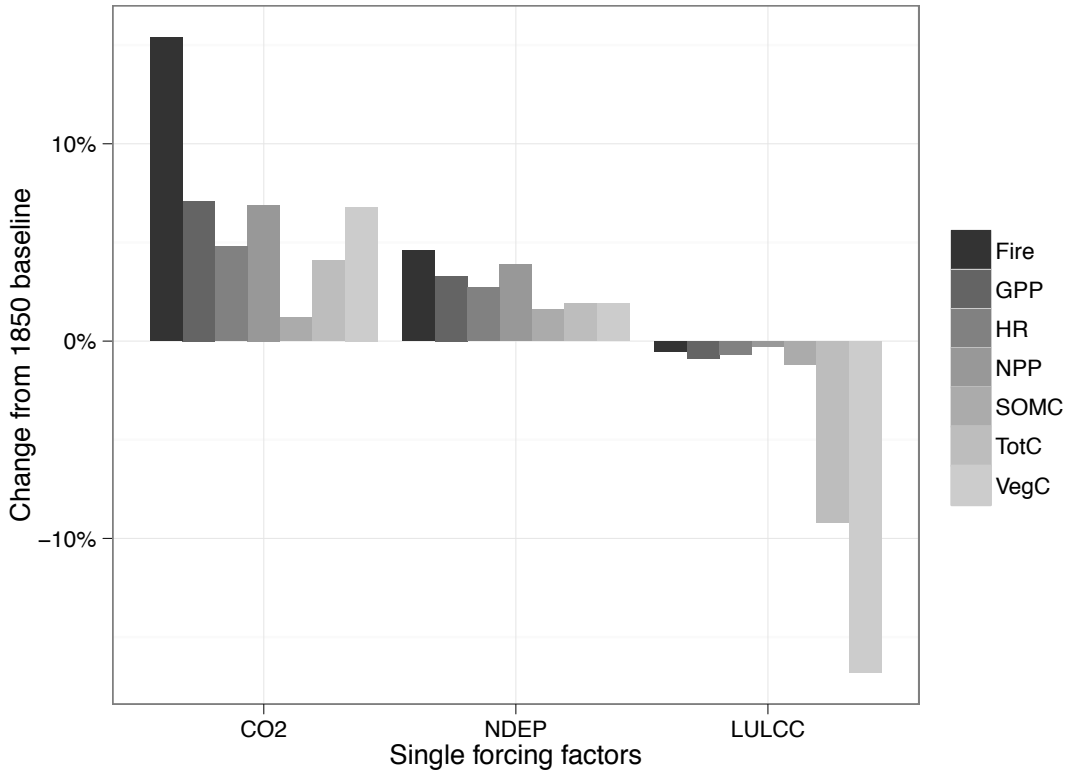

Figure 3. GCAM model output (energy derived from bioenergy by region of the world) in two model runs, the RCP4.5 control and a coupled CLM-GCAM run using carbon stocks as a coupling mechanism. In this latter case the model diverged sharply and unrealistically from the RCP4.5 control, because the vulnerability of C stock data to disturbance effects triggered a feedback loop in GCAM. Data are from model year 2065, when the run was stopped.

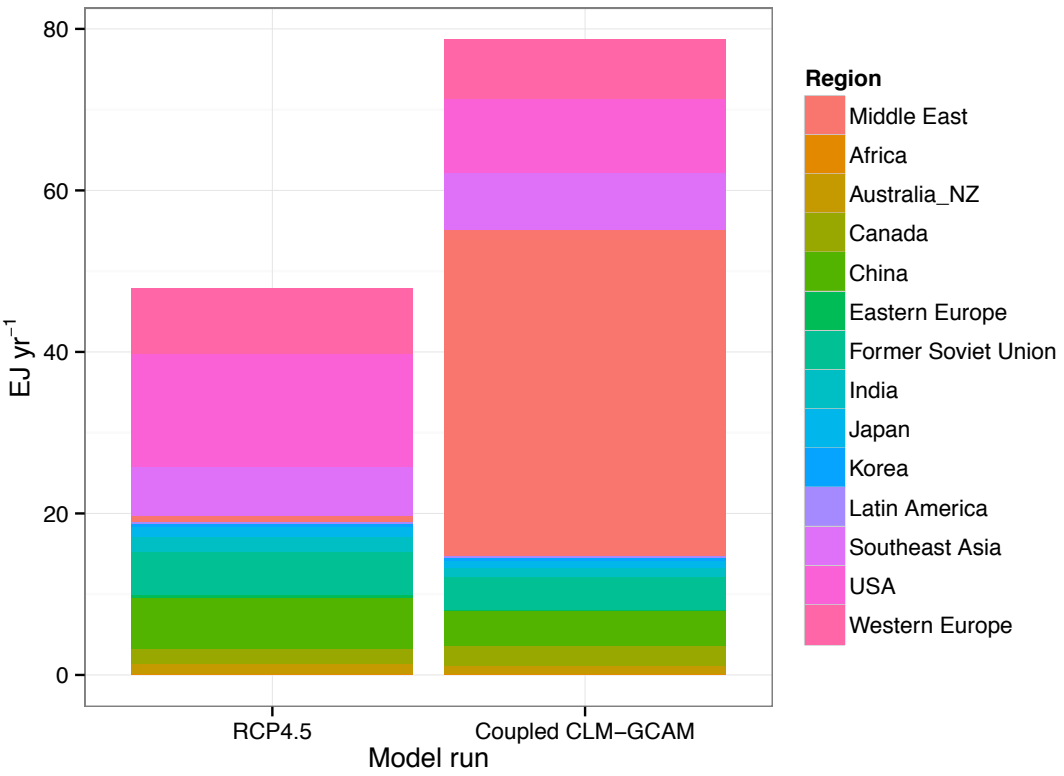

679 **Figure 4.** Relationship between net primary production (NPP, 2005-2009) to biomass
680 (2090-2094) in CLM for crops, grasses, shrubs, and trees; cf. **Table 2**. Lines show best-
681 fit linear regressions. Results are from the E1 and E2 simulations in **Table 1**.

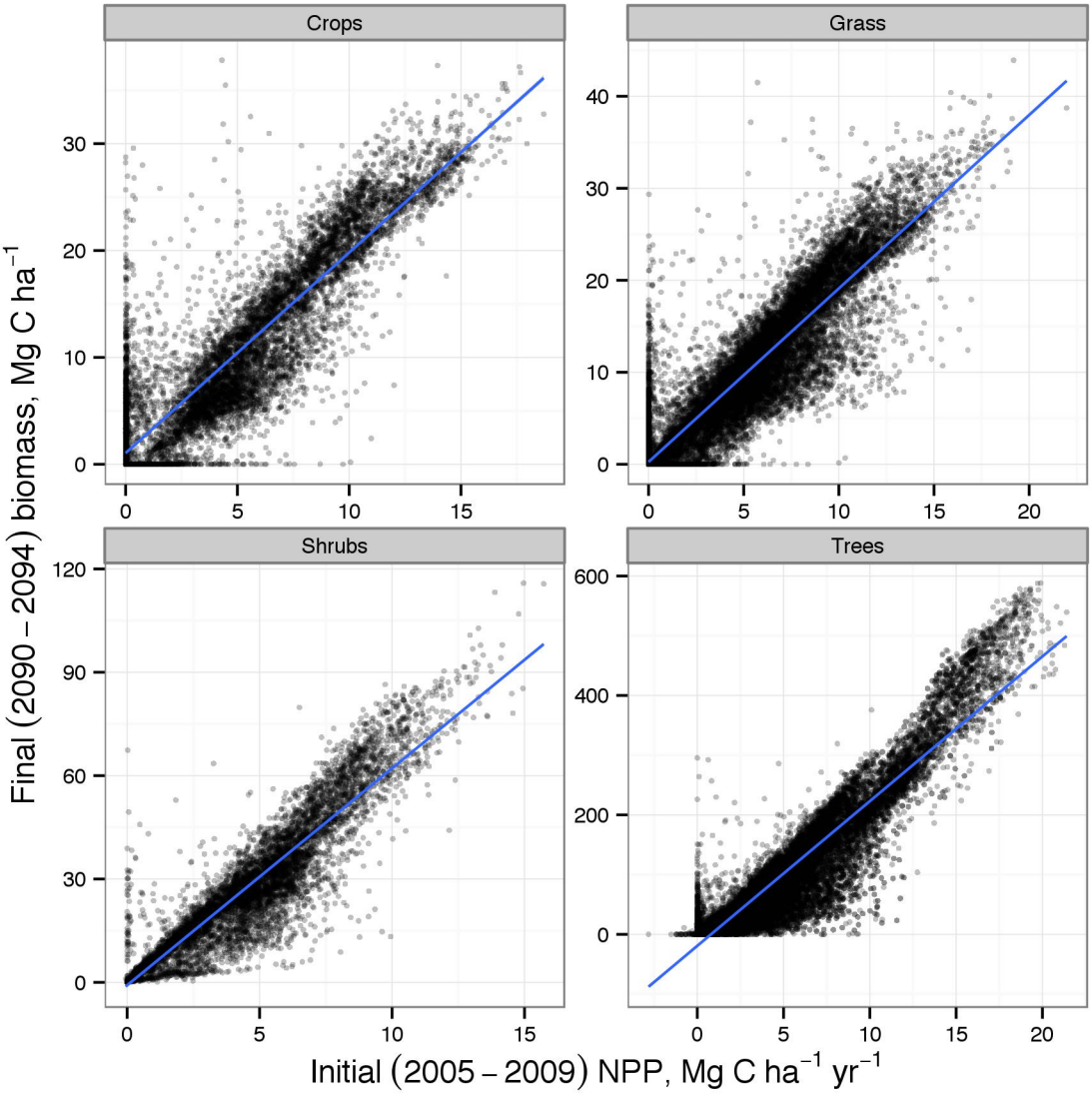

682

683

Figure 5. Monte Carlo simulation M1 (cf. **Table 1**) examining how well an outlier test can distinguish between climate and land use change (LUC) signals when passing data from CLM to GCAM. Contour lines (every 25%) show error between the inferred climate change signal and the known (artificial) signal as increasing numbers of cells (y axis) are perturbed by LUC with increasing intensity (x axis). LUC intensity is shown as the ratio of perturbed cells' equilibrium C to unperturbed cells: a doubling (e.g. transitioning from crop to young forest) is an effect of 2.0, a halving as 0.5, etc.